Journal of Zoology

Journal of Zoology. Print ISSN 0952-8369

Dorsal fin function in spiny dogfish during steady swimming

A. Maia & C. A. Wilga

Department of Biological Sciences, College of the Environmental and Life Sciences, University of Rhode Island, Kingston, RI, USA

Keywords
elasmobranchs; functional morphology; locomotion; kinematics; muscle activity; median fins.

Correspondence
Anabela Maia, Department of Biological Sciences, Eastern Illinois University, 600 Lincoln Ave, Charleston, IL 61920, USA.
Email: amresendedamaia@eiu.edu

Editor: Andrew Kitchener

Received 21 September 2013; revised 4 August 2015; accepted 2 September 2015

doi:10.1111/jzo.12300

Abstract

Dorsal fins of actinopterygian fishes are known to function to varying degrees as stabilizers and as propulsive elements that augment thrust from the caudal fin. However, little is known about the ability of elasmobranchs to control three-dimensional conformation of the dorsal fins during swimming, which may alter the force balance during locomotion. In this study, dorsal fin function was investigated in spiny dogfish, *Squalus acanthias*, swimming steadily at 0.5 and 0.75 BL s^{-1}, using three-dimensional kinematics and electromyography. Points on the dorsal and caudal fins were tracked in dorsal and lateral views with dual high-speed video at 125 f s^{-1}. Electrodes were implanted in three points along each dorsal fin muscle and in the adjacent red epaxial muscle. Conformational changes were detected in both dorsal fins at both speeds. Speed was found to influence lateral displacement of the first dorsal fin relative to trunk undulation, with larger magnitudes at 0.5 BL s^{-1}. The first dorsal fin oscillates at a different phase lag than predicted by position on the body, while the second dorsal fin moves in synchrony with the axial musculature. Muscles of the first dorsal fin show synchronous bilateral activation, while there is no clear pattern in the second dorsal fin. This study provides evidence that spiny dogfish control movements of the first dorsal fin during steady swimming to stabilize body position. In contrast, the second dorsal fin appears to be capable of thrust generation. Thus, there is a dual dorsal fin function in spiny dogfish during steady swimming.

Introduction

Studies on actinopterygian fishes have revealed that the dorsal and anal fins can function as thrusters or stabilizers during steady swimming (Drucker & Lauder, 2005; Standen & Lauder, 2005, 2007). In bluegill sunfish, the dorsal and anal fins act as thrusters complementing the role of the caudal fin (Drucker & Lauder, 2005; Standen & Lauder, 2005). In this species, the anal and dorsal fins extend to the caudal peduncle and move in phase with the adjacent trunk (Drucker & Lauder, 2005; Standen & Lauder, 2005). In another actinopterygian fish, the brook trout, the main dorsal fin is placed more anteriorly in the body and functions as a stabilizer during steady swimming by moving out of phase of the adjacent trunk (Standen & Lauder, 2007). However, the muscular and skeletal arrangement in the dorsal fins of actinopterygian fishes is very different from that of chondrichthyan fishes. Actinopterygian fishes have fin rays composed of two distally fused hemitrichia with muscles attached laterally at the base (Geerlink, 1987). Contraction of muscles on one side causes the hemitrichia to slide and places the other side in tension, bending the fin ray towards the contracted muscle (Lauder, 2006). In contrast, the musculoskeletal elements in the dorsal fins of squalean sharks, like the spiny dogfish, are relatively simple. The skeletal organization of the dorsal fins consists of single or multiple basal cartilages inserting into the midline of the trunk with radials and ceratotrichia supporting the fin web (Benzer, 1944; Compagno, 1999; Maia & Wilga, 2013*b*). The musculature of the dorsal fins consists of a single mass of angled posteriorly parallel fibers, originating from the stratum compactum of the skin overlying the trunk just below the fin and inserting into the connective tissue attached to the ceratotrichia (Liem & Summers, 1999; Maia & Wilga, 2013*b*; Shirai, 1996; Fig. 1).

Squalus acanthias (Linnaeus, 1758; Order Squaliformes, Family Squalidae), commonly known as spiny or piked dogfish, inhabit the coastal and continental shelf waters from temperate to subarctic regions (Compagno, 1984). Spiny dogfish have a large epicaudal lobe in the caudal fin, lack anal fins, and swim using the body and caudal fin in an anguilliform mode of locomotion (Simanek & Thomson, 1977; Maia, Wilga & Lauder, 2012). Spiny dogfish were chosen as a model for this study as a representative of basal elasmobranchs (Squaliformes) that retains the ancestral chondrichthyan character of spines in both dorsal fins (Schaeffer & Williams, 1977). In addition, *Squalus* have two different sized dorsal fins with a larger and more anterior placed first dorsal fin and a smaller second dorsal fin closer to the caudal peduncle (Compagno, 1984; Maia & Wilga, 2013*b*).

Much progress has been made on the functional analysis of whole body kinematics, tail and pectoral fins of sharks

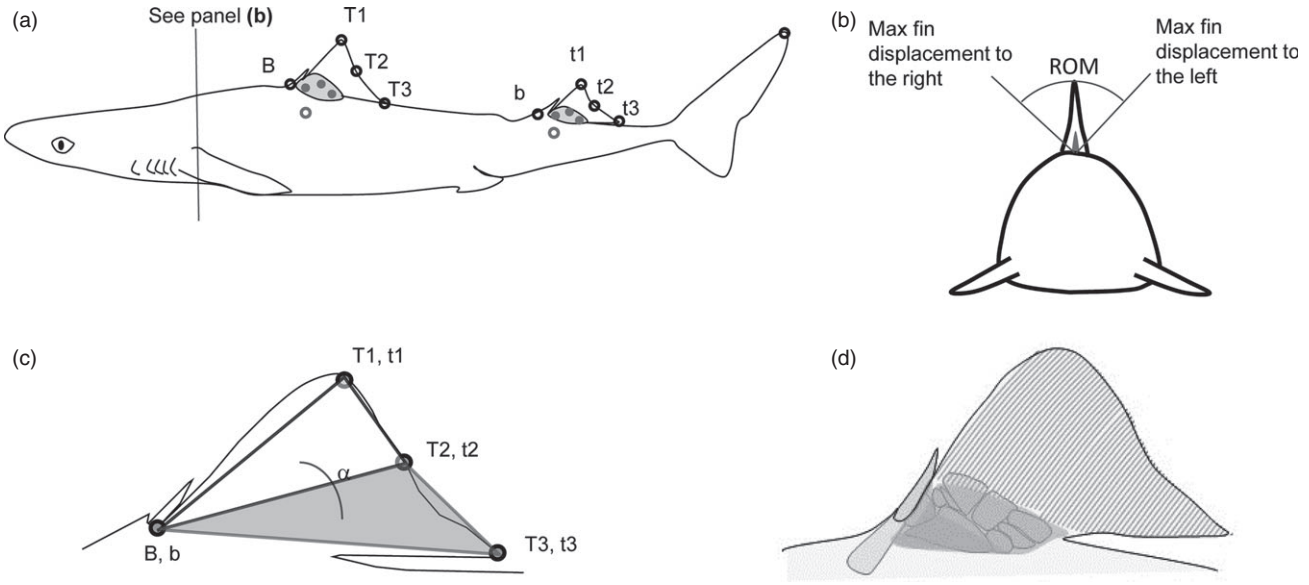

Figure 1 Dorsal fin arrangement and landmark position. (a) Landmarks used to determine the three dimensional kinematics of spiny dogfish dorsal fins during steady swimming (black dots) and electrodes implanted (gray dots). The open gray circles refer to the electrodes implanted only unilaterally; (b) frontal section at the level of the dashed line in a to illustrate the range of motion (ROM) measurement; (c) detail of first dorsal fin with leading edge (white) and trailing edge (shaded) planes highlighted used to measure the angle α represented by the arc. Uppercase letters refer to landmarks on the first dorsal fin (B-base, T1-distal tip of the fin, T2-mid-point between T1 and T3, and T3-trailing edge tip) and lowercase letters refer to the second dorsal fin landmarks (b-base, t1-distal tip of the fin, t2-mid-point between t1 and t3, and t3-trailing edge tip); (d) muscoskeletal arrangement of the dorsal fin, the cartilaginous elements are outlined, the parallel lines represent the ceratotrichia and the shaded area represent the dorsal fin muscle, which covers most of the skeletal elements, and the ligament, the anterior triangle connected to the spine.

(Simons, 1970; Webb & Keyes, 1982; Ferry & Lauder, 1996; Wilga & Lauder, 2000, 2001, 2002, 2004; Donley & Shadwick, 2003, 2005; Flammang, 2010). However, few studies have investigated the functional morphology of the dorsal fins in particular (Maia & Wilga, 2013*a*). Early manipulative studies investigated dorsal fin function in elasmobranchs, using models in a wind tunnel and suggested that median fins function to prevent roll (Harris, 1936). The purpose of this study is to investigate the function of the dorsal fins during steady swimming in a squalean shark species using three-dimensional kinematics and electromyography (EMG). We hypothesize that the dorsal fins of squalean sharks with the basal character of anteriorly positioned spines will have reduced mobility and will function as stabilizers as predicted by Harris (1936). Therefore, we expect the dorsal fins to move independently and with no relationship to trunk movement to adjust body position. Muscle activity is expected to be bilaterally synchronous in order to stiffen the fin.

Materials and methods

Experimental subjects

Four spiny dogfish were obtained from the Graduate School of Oceanography (URI) trawl cruises in Narragansett Bay. Individuals were kept in a 8900 L round tank (3 m diameter and 1.20 m high). The tank was maintained at 32 psu salinity, 18°C (±1°C) and a 12:12 h light:dark cycle. Sharks were fed every other day on a natural diet of fish (*Scomber* sp., *Clupea* sp.) and squid (*Illex* sp.). Two female and two male mature individuals were used with speed reported relative to body length (range 56 to 86 cm, $\bar{x} = 72.5 \pm 14.8$ cm).

3D kinematics

Four spiny dogfish were placed in a flow tank (Rolling Hills Research, El Segundo, CA, USA, Model 1520, working section 1.5 m length × 0.5 m height × 0.38 m width) and trained to maintain steady, rectilinear swimming at speeds of 0.50 and 0.75 BL s^{-1}. Reflective metal markers (2 mm diameter, approximately 2 mg each) were fixed onto the dorsal and caudal fins with cyanoacrylate glue to track fin movement (Fig. 1a). These markers were used to define four landmarks on each dorsal fin [base (B, b), tip of the fin (T1, t1), trailing edge (T3, t3) and mid-point between the tip and the trailing edge (T2, t2)]. Uppercase is used to denote landmarks on the first dorsal fin and lowercase to denote landmarks in the second dorsal fin. The shark was anesthetized with MS222 (1.75 g in 20 L for 5 min), markers were placed in under 30 min and the animal was allowed to recover for 90 min, after which the shark was fully recovered as evidenced by regular ventilation rate, normal swimming activity and tank exploratory behaviours. Two high-speed video cameras

(125 frames s^{-1}; Photron FastCam, Photron, San Diego, CA, USA) recorded simultaneously lateral and dorsal views. Experiments were conducted at holding tank temperature (18°C). Videos from the two lateral views were calibrated to generate 3D coordinates following Standen & Lauder (2005). The two camera views were calibrated using DLTcalibration.m in Matlab (Hedrick, 2008).

We analysed four independent randomly chosen tail beats per individual and speed from sequences where the animal was steadily swimming for at least six tail beats using Photron Motion Tools 1.0.1.3. (Photron, San Diego, CA, USA) Tail beat cycles were defined from the point of maximum excursion of the tail to one side and return to that same side after passing the midline twice. The snout and the tip of the upper lobe of the caudal fin were digitized in every frame and tail amplitude and period were calculated. Reflective markers on the fins were tracked in every frame and 3D coordinates were used to calculate kinematic variables: excursion rate, total displacement, and time of maximal displacement to each side. Lateral displacement of each fin landmark was corrected by subtracting the coordinates of the base (B, b) of each fin. Range of motion (ROM) of the fins, defined as the angle between the maximum displacement to one side and the maximum displacement to the other side during a single tail beat (Fig. 1b), was calculated relative to the earth and shark referentials. For this, we used the angle between the plane defined by the following landmarks: anterior portion of the fin base (b, B), tip of fin (T1, t1) and trailing edge (T3, t3) at the point of maximum displacement to one side and the same plane at maximum displacement to the opposite side (Ferry & Lauder, 1996). The fin was further divided into two smaller triangles representing the leading edge and trailing edge (Fig. 1c) and the angle between these two triangles was used to test for conformational changes within the fin for each tail beat, that is, a measure of cupping. In order to test the phase lag of each fin tip in relation to the body motion, we compare the movement of the fin tip (T1, t1) to the local propagation of the body wave. The locomotor wave characteristics were calculated by tracking the base of the first and second dorsal fins. The phase lag was calculated by determining the horizontal distance between the base of the fin (B, b) and the tip of the fin (T1, t1) and then dividing that distance by the wavelength of the locomotor wave and multiplying by the wave period (Standen & Lauder, 2005). From these data we were also able to derive the predicted timing of maximum fin tip displacement which was compared to the observed timing of maximum lateral displacement. In reality this is the same as comparing the movement of the fin tip to the movement of point directly underneath it. However, most of the time, this point cannot be easily tracked in the dorsal view since it is covered by the flexed fin. This approach assumes that the fins are stiff structures, a good approximation for the anterior portion of the dorsal fins in this species due to the presence of the dorsal spines. It is predicted that passive structures match the expected phase lag, while active structures should not.

Paired *T*-tests were used to test for differences in caudal fin amplitude and frequency at the two swimming speeds, differences between fin landmarks and the respective base and between expected and predicted timing of maximum displacement, that is, phase lag (Zar, 2009). If the data were not normally distributed, Mann–Whitney tests (Zar, 2009) were used. Two-way ANOVAs were used to test for differences in excursion rates, angles, and timing of maximal displacement between fins and speeds (Zar, 2009). Bonferroni corrections were used to compensate for the lack of independence of the variables being tested (Zar, 2009). When normality tests failed, ANOVA on ranks followed by Dunn comparison tests were used (Zar, 2009).

Muscle activity

Three sharks were anesthetized, using MS222 and intubated with seawater with MS222 at a diluted concentration (1.75 g in 20 L for 5 min) for the duration of the surgery (<60 min). Bipolar stainless steel electrodes were implanted bilaterally, using a 25-gauge needle into three locations along each dorsal fin muscle: leading edge, middle of the fin and trailing edge locations (Fig. 1a). Two additional electrodes were implanted on the red epaxial muscle below each fin only on the left side (Fig. 1a). The shark was allowed to recover in the flow tank for 2 h after surgery. After 1 h, the animal was fully awake and swimming normally. The temperature in the experimental tank was kept at the same temperature as the holding tank (18°C). EMG signals were recorded with differential amplifiers 1700 (AM Systems, Sequiem, WA, USA) at 100 kHz, with a low-pass filter setting of 10 kHz and a high-pass filter setting of 3 Hz. Analog muscle signals were converted into digital, using a PowerLab/16sp (ADInstruments, Colorado Springs, CO, USA) and stored in a computer. EMG signals were filtered digitally with a notch filter of 50 Hz to reduce acoustic noise from the propeller. We recorded the animal swimming without the tank on and filtered the signals using the same procedure to make sure that there was no activity being eliminated by the digital filter. Waveform analyses were conducted, using Chart software (v.5.4.2; ADInstruments) for four trials for each individual. To determine onset and offset of EMG activity, a rectified, integrated EMG signal was used. Onset and offset were then obtained as the time when the rectified and integrated signal reached 2.5 times the baseline value or when it dropped to that same threshold, respectively (Roberts *et al.*, 2007). Red epaxial muscle near the first dorsal fin was used as the reference for all the muscles implanted. The magnitude of an individual muscle burst was determined relative to the maximum peak for that muscle implant. Duty cycle was defined as the percentage of the duration of the cycle in which each muscle was active. A cycle was defined from onset of the reference implant to the next onset of the same implant after a baseline value.

All summary statistics are reported as mean ± standard deviation. To test for the effect of fin (1st and 2nd dorsal), a two-way mixed model analysis of variance was performed, with individual as the random effect and fin as the fixed effect (Zar, 2009). Paired *T*-tests were used to test for differences between left and right muscle pairs (Zar, 2009).

Results

3D kinematics

Spiny dogfish swam by body-caudal undulations with motion of the dorsal fins (Supporting Information Movie S1). Increase in swimming speed was accomplished by increasing tail beat frequency (0.88 s^{-1} at 0.5 BL s^{-1}; 1.20 s^{-1} at 0.75 BL s^{-1}, $t = -6.265$, d.f. = 30, $P < 0.05$), while maintaining a constant tail beat amplitude (19.6 cm at 0.5 BL s^{-1}; 17.1 cm at 0.75 BL s^{-1}, $t = 1.695$, d.f. = 30, $P = 0.100$). Despite the different shark sizes, individual did not influence tail beat amplitude. Most of the movement of the two dorsal fins occurred in the horizontal plane with a lesser vertical component at both speeds (Fig. 2).

The first dorsal fin lagged the adjacent trunk at 0.5 BL s^{-1} by a mean of 269 ms, which is longer than the predicted mean value of 128 ms ($H = 17.41$, d.f. = 2, $P < 0.05$). However, the phase lag of the first dorsal fin did not differ from the expected at a higher speed and the phase lag of the second dorsal fin did not differ from the expected at either speed. Representative traces of predicted and observed movement of the tip show clear phase shifts in the timing of the first dorsal fin (Fig. 3).

Mean lateral displacement of fin landmarks relative to the fin base at the lower speed was higher at points T2 ($T = 204$, $n = 16$, $P < 0.05$) and T3 ($T = 185$, $n = 16$, $P < 0.05$) (Fig. 4a). The displacement of points on the second dorsal fin did not differ from that of the base for either speed (Fig. 4a and b). At 0.5 BL s^{-1}, all landmarks on the first dorsal fin showed larger displacement relative to the body than the more posterior points in the second dorsal fin ($H = 98.89$, d.f. = 11, $P < 0.05$). Displacement of the points on the second fin was on average lower than the base of the fin (Fig. 4a and b).

The differences in timing of the maximum lateral displacement of the two dorsal fins among tail beat cycles (Figs 3 and

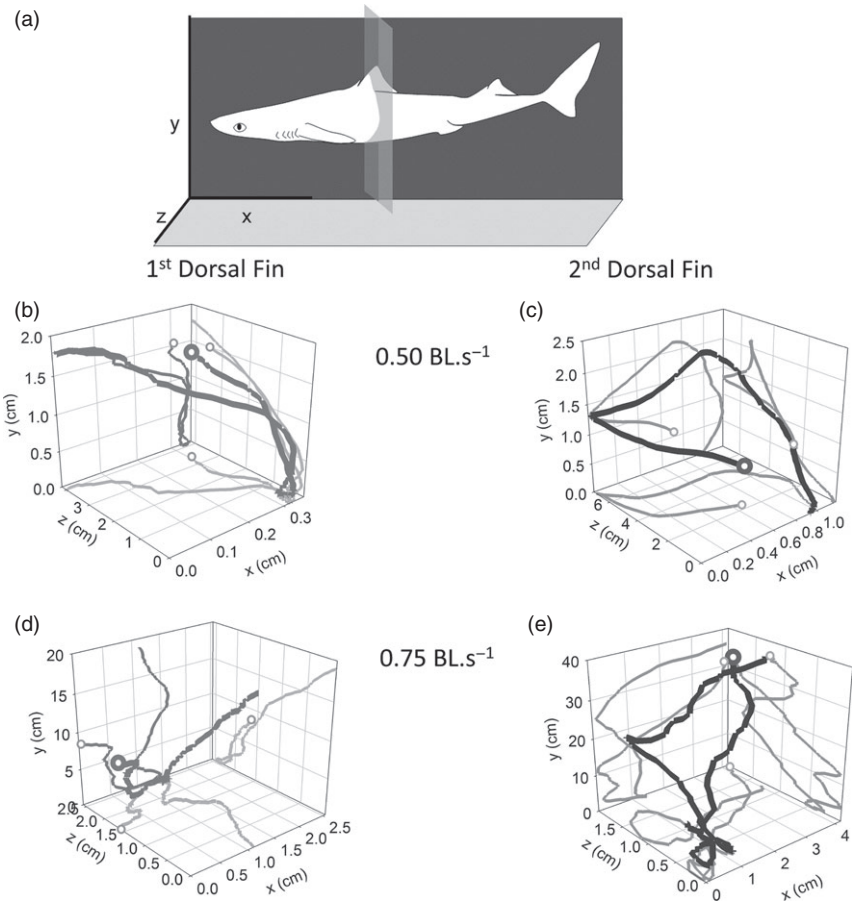

Figure 2 Representative plots of three-dimensional (3D) dorsal fin kinematics during the one tail beat corrected by body displacement. (a) Sagittal, transverse, and frontal planes analyzed that intersect the fish at the dorsal fins; (b) Decomposition of 3D kinematics of the first dorsal fin tip at 0.5 BL s^{-1}; (c) Decomposition of 3D kinematics of the second dorsal fin tip at 0.5 BL s^{-1}; (d) Decomposition of the 3D kinematics of the first dorsal fin tip at 0.75 BL s^{-1}; and (e) Decomposition of the 3D kinematics of the second dorsal fin tip kinematics at 0.75 BL s^{-1}. Darker lines indicate 3D movement of the fin, while lighter lines indicate decomposition of fin movement into three planes. Open circles indicate the beginning of the tail beat cycle. Note that and the z axes have higher magnitudes, which relate to the higher range of motion in the xoy plane.

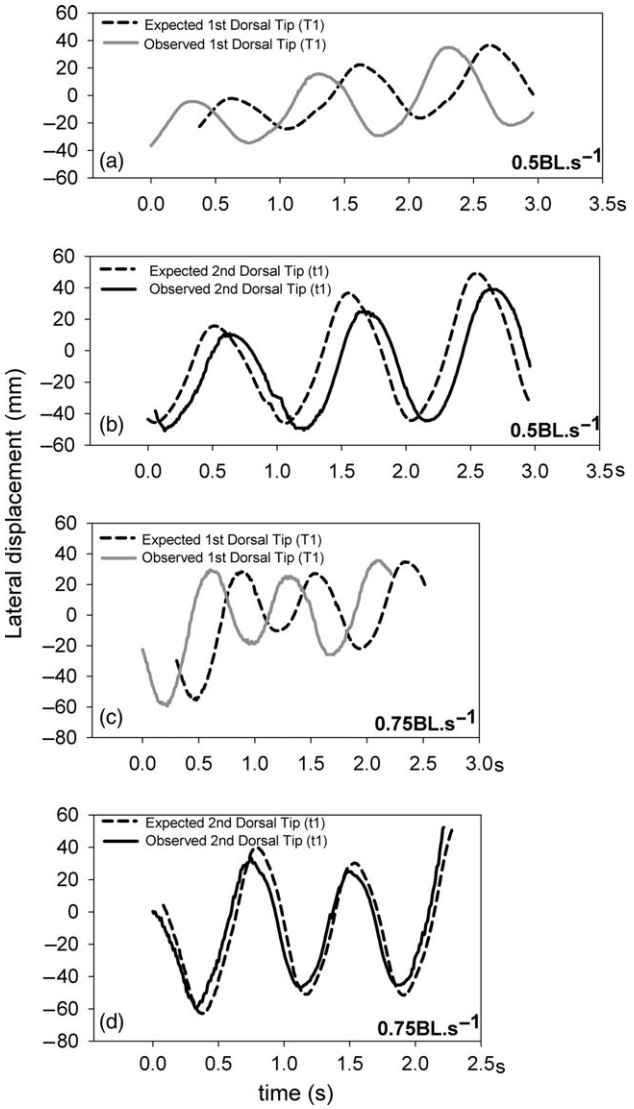

Figure 3 Representative plots of lateral fin displacement over time for the (a) observed (solid line) first dorsal fin tip and expected (dashed line) dorsal fin tip displacement based on position at 0.5 BL s^{-1}; (b) observed (solid line) and expected (dashed line) second dorsal fin tip at 0.5 BL s^{-1}; (c) observed (solid line) and expected (dashed line) first dorsal fin tip at 0.75 BL s^{-1}; and (d) observed (solid line) and expected (dashed line) second dorsal fin tip at 0.75 BL s^{-1}.

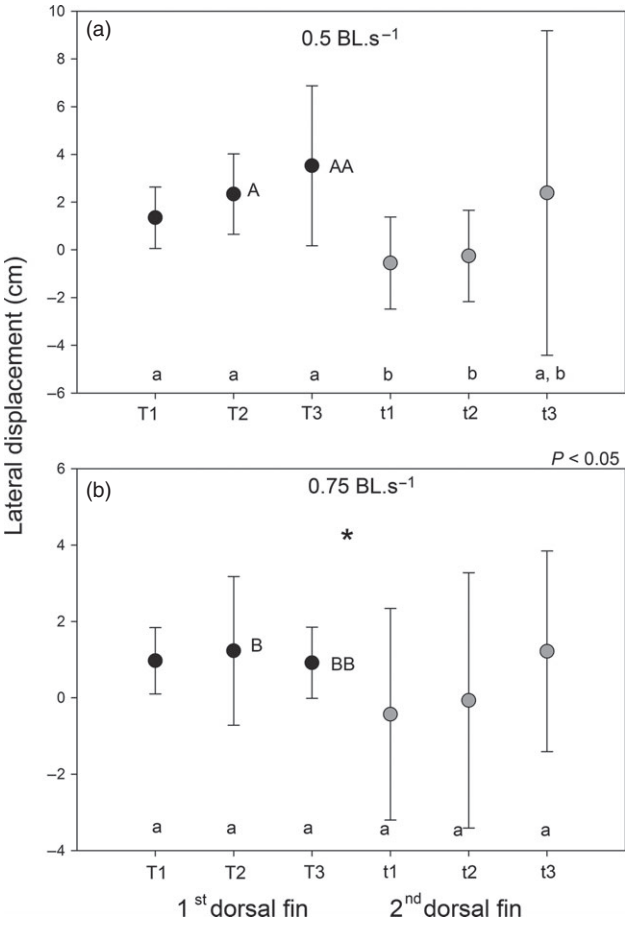

Figure 4 Plot of mean lateral displacement of fin landmarks for all trials corrected by the movement of the base of each fin (T lines represent standard deviation), at 0.5 BL s^{-1} (a) and 0.75 BL s^{-1} (b). Negative values represent landmarks moving less than the base. Fin landmarks on the first dorsal fin (B, T1, T2, T3) and second dorsal fin (b, t1, t2, t3) are: B, b-base, T1, t1- distal tip of the fin, T2, t2-mid-point between T1, t1 and T3, t3, and T3, t3-trailing edge tip). Lower case letters represent statistical differences among fin landmarks, upper case letters statistical differences between speeds for each landmark.

5) indicated that the first and second dorsal fins were out of phase with one another. In addition, at a lower speed, the first dorsal fin was maximally displaced to the right or left side in the middle of a tail beat cycle and this could not be predicted by speed or phase of the tail beat.

The ROM of the dorsal fins varied with fins but not with the individual or speed, in the earth frame of reference (Table 1). ROM was larger for the second dorsal fin (43.9°) than for the first fin (18.7°). There were no differences in ROM in the shark frame of reference. Variation in the angle between leading and trailing edge of the two dorsal fins differ with fin and swimming speed. The angle between these two portions of the fin was higher for the second dorsal fin (first dorsal fin 18.7°, second dorsal fin 63.2°, Table 2). Higher speeds also produced higher angles between anterior and posterior portions of the fin (56.2° at 0.75 BL s^{-1}, 37.4° at 0.5 BL s^{-1}).

Muscle activity

All the muscles examined from the dorsal fin and adjacent musculature were active during the majority of a cycle (Figs 6 and 7). Muscle activity among the three implants on the same side was similar for onset and duration variables. However,

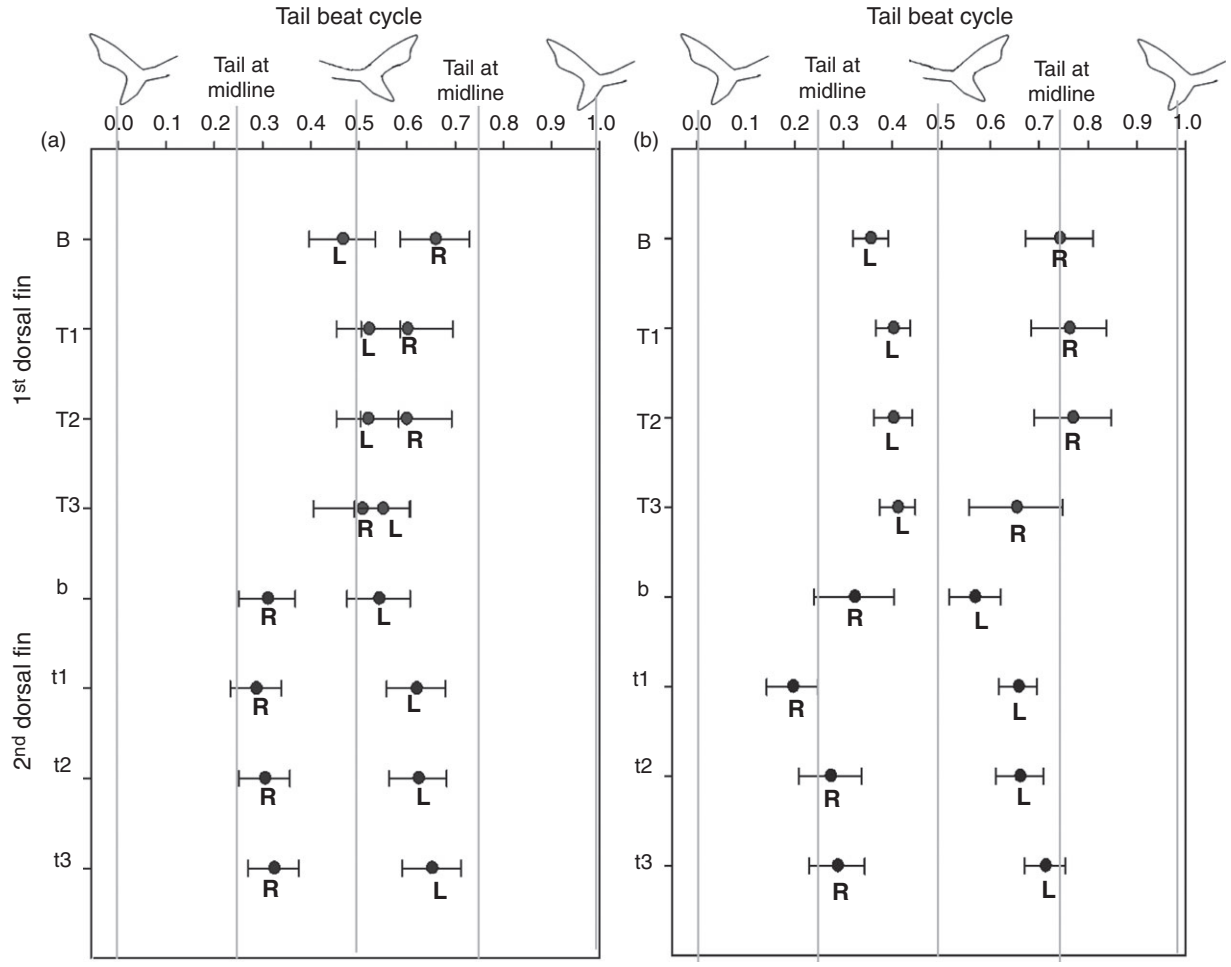

Figure 5 Time as a proportion of the tail beat cycle (from maximum excursion to the left to the consecutive maximum excursion to the left) for maximum lateral displacement to the right (R) and to the left (L) for each dorsal fin landmarks at 0.5 BL s^{-1} (a) and 0.75 BL s^{-1} (b) (circles represent means and lines standard deviation). Uppercase letters refer to landmarks on the first dorsal fin and lowercase refers to the second dorsal fin (B, b-base, T1, t1- distal tip of the fin, T2, t2-mid-point between T1, t1 and T3, t3, and T3, t3-trailing edge tip).

Table 1 Angles for the range of motion in the earth referential for the different factors and *P*-value results from the three-way ANOVA

Variable	Mean (°)	*P*
Fin		
1st Dorsal	18.72	<0.001
2nd Dorsal	43.90	
Speed		
0.5 BL s^{-1}	36.13	0.068
0.75 BL s^{-1}	26.49	
Individual		
1	27.91	0.24
2	35.27	
3	37.52	
4	24.56	

Table 2 Bending angles between leading and trailing edge portions of the fin for the different factors and *P*-value results from the three-way ANOVA

Variable	Mean (°)	*P*
Fin		
1st Dorsal	30.43	<0.001
2nd Dorsal	63.21	
Speed		
0.5 BL s^{-1}	37.40	0.002
0.75 BL s^{-1}	56.23	
Individual		
1	55.02	0.032
2	50.90	
3	49.65	
4	31.71	

sporadically, the timing and magnitude of muscle activity among the three implants on the same side of each fin were different.

Muscle activity in the dorsal fins during steady swimming is cyclical (Fig. 6). Overall burst duration was shorter at the higher speed ($U = 8754$, $P < 0.05$, Fig. 7). Duty cycle for all

muscles tested ranged between 24 and 52% and did not vary with swimming speed. Burst duration was also similar among all muscles implanted for each speed. Paired *t*-tests (between the left and right sides of the dorsal fin muscle with all the muscles from for each fin) show similar onset and offset for the first dorsal fin for both speeds. Similarly, tests for the second dorsal fin revealed no differences between left and right activation patterns, however there is a tendency for left and right alternated muscle activation (Fig. 7). No differences in magnitude were detected among implants within muscles, speeds, or individuals.

Discussion

Spiny dogfish are able to control both dorsal fins actively during steady swimming as evidenced by three-dimensional conformational changes and cyclic muscle activity. Despite the simple musculoskeletal arrangement, squalean shark dorsal fins are more than the passive stabilizing structures hypothesized by Harris (1936). The skeletal elements and ceratotrichia in conjunction with the fin muscles (Fig. 1d) might provide a functional analog to the sliding fin rays and dorsal inclinator muscles of teleosts, where independent fin ray curvature is achieved (Standen & Lauder, 2005). In bony fishes, muscles attached to each hemitrichium cause sliding and bending towards the muscle being activated (Standen & Lauder, 2005). In spiny dogfish, the curvature can be achieved by the asymmetric contraction of dorsal fin muscles in conjunction with the arrangement of the ceratotrichia over the skeletal elements (Maia & Wilga, 2013*b*).

Differences in lateral displacement and phase lag indicate that the first dorsal fin of spiny dogfish moves independently from the body axis during steady swimming, and this was more pronounced at low speeds. Spiny dogfish are actively moving the first dorsal fin independently of the trunk, which is corroborated by muscle activity that differs from the adjacent epaxial muscle. Greater lateral movement of the first dorsal fin at low speed indicates that the fin is functioning to increase

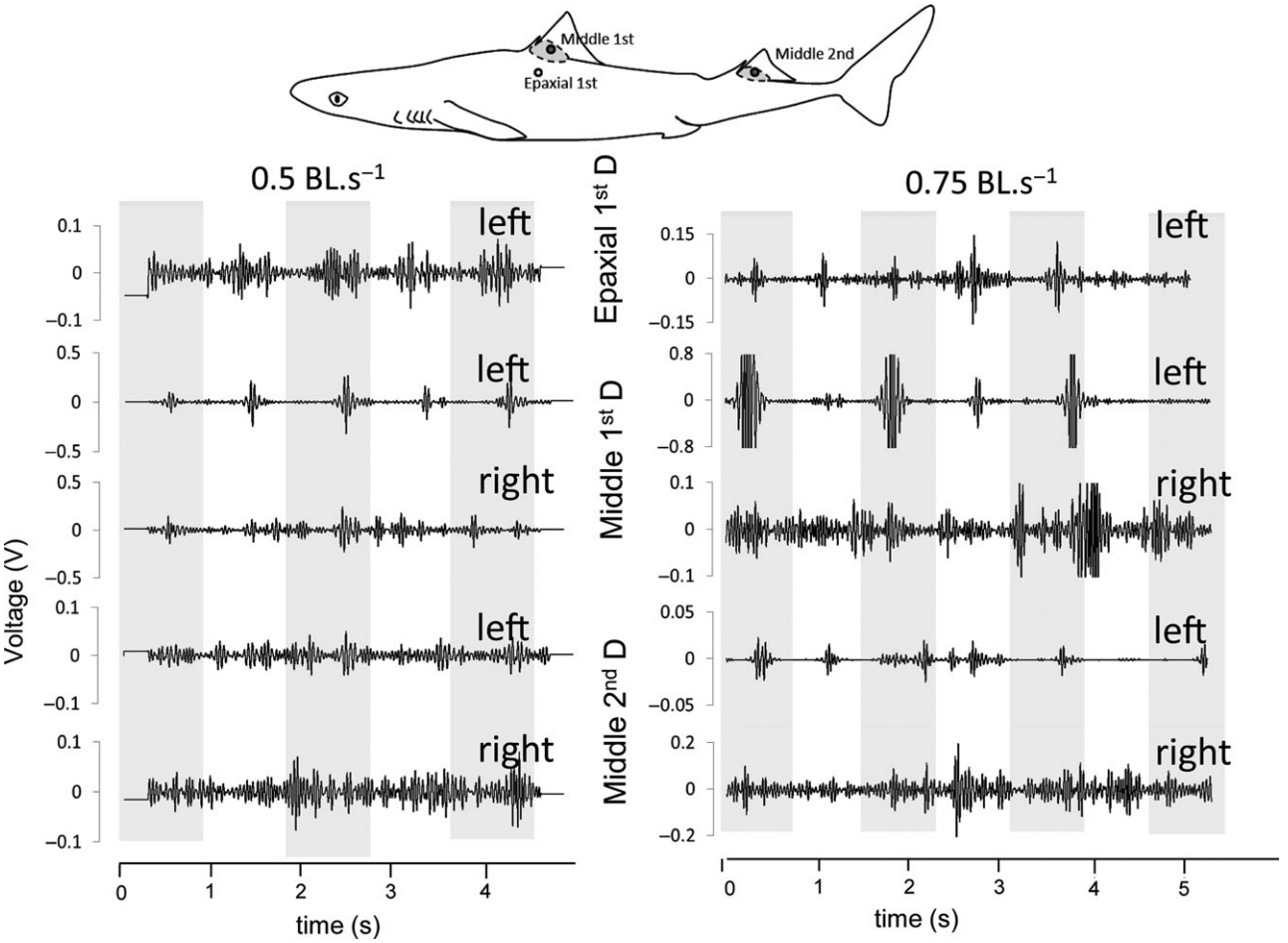

Figure 6 Representative electromyograms of dorsal fin activity in spiny dogfish during consecutive tail beats of steady swimming at 0.5 BL s^{-1} (five tail beats) and 0.75 BL s^{-1} (seven tail beats). For clarity purposes only the electrode placed in the middle position of each dorsal fin muscle is represented; shaded box indicates a cycle corresponding to a tail beat. Black traces, left epaxial activity from the first dorsal fin (reference electrode); light gray traces, left dorsal fin muscles; dark gray traces, right dorsal fin muscles.

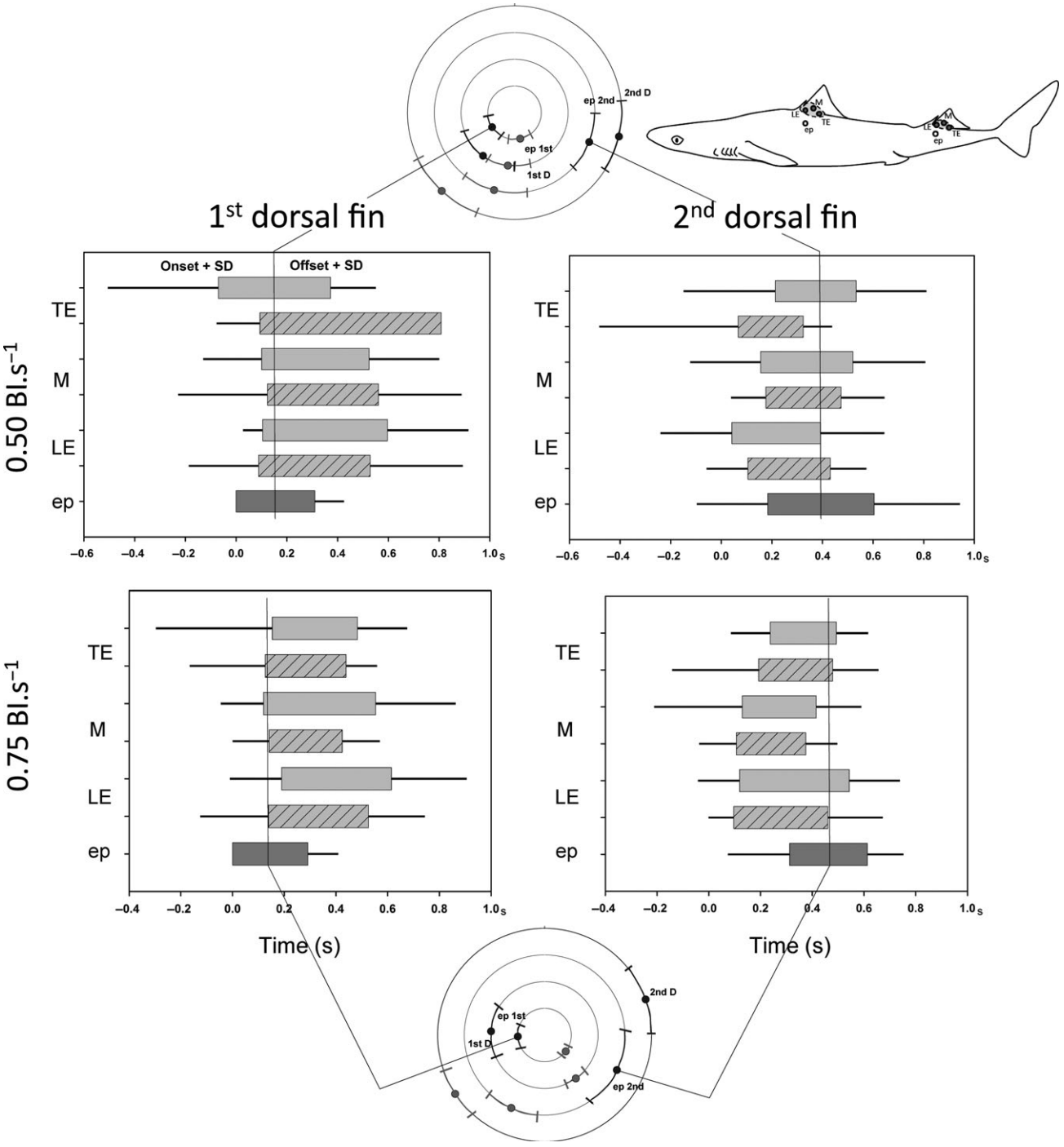

Figure 7 Temporal variables (onset and offset, mean and standard deviation) for dorsal fin muscle activation in spiny dogfish during steady swimming for all individuals and trials combined (ep, left red epaxial; LE, leading edge; M, middle; TE, trailing edge; striped bars represent muscles on the left side and solid bars represent muscles on the right side). For reference, circular plots display the average (and standard error) maximum displacement of the body (epaxial – ep) and of the dorsal fins (1st dorsal fin tip – 1st D, 2nd dorsal fin tip – 2nd D) to the left (black) and to the right (gray). Maximum displacement of the body is lined with peak contraction of the epaxial.

stability, similar to the dorsal fin function of brook trout (Standen & Lauder, 2007). In addition, unpredictability in the position of the first dorsal fin within a tail beat cycle (Fig. 5) indicates functional independence from axial movement and suggests that the dorsal fin may function to counteract unsteady movements created by the animal undulating in the

flow. As it would be expected in a stabilizing structure, the dorsal fin muscles are active simultaneously on both sides. This can contribute to increased stiffness and allow the fin to react to the incoming flow. Muscle activity that results in increased fin stiffness has been observed in pectoral fins of sturgeon (Wilga & Lauder, 1999), in the radialis muscle of shark tails (Flammang, 2010) and in the hemitrichia of actinopterygians (Arita, 1971).

One of the most common disturbances during locomotion is rotation around the axial body of the fish, referred to as roll (Webb, 2006). Teleost fishes compensate for roll disturbances by making positional adjustments with the median and paired fins (Webb, 2006; Tritico & Cotel, 2010). The relevance of roll instabilities is evident by the shorter latency period in correcting roll when compared to yaw and pitch perturbations (Webb, 2004). Disturbances due to roll are more common at low speeds and in fusiform-shaped bodies (Fish, 2002). This supports the role of the dorsal fins in roll prevention as was hypothesized in a study, using shark models in a wind tunnel (Harris, 1936). The high risk of roll of a shark body (Fish, 2002), appears to be compensated by stabilization through an anterior placed first dorsal fin in pelagic shark species (Lingham-Soliar, 2005). In white sharks, the first dorsal fin is thought to function as a dynamic stabilizer during steady swimming based on dermal fiber arrangement (Lingham-Soliar, 2005). The tightly packed and layered dermal arrangement with fibers in opposing directions could induce stiffness through increased internal hydrostatic pressure (Lingham-Soliar, 2005). A similar arrangement is present in the first dorsal fin of spiny dogfish with the spine braced by a ligament on both sides covering part on the dorsal fin muscle fibers (Maia & Wilga, 2013*b*). This spine–ligament combination confers stiffness to the anterior portion of the dorsal fin (Maia & Wilga, 2013*b*). This ligament is larger and tighter in the first dorsal fin than in the second (A. Maia, pers. obs.). Thus less movement is expected in the anterior portion of the first dorsal fin.

In different fish species, stabilization or trimming is accomplished by means of median and paired fins (Harris, 1937). In sharks, the pectoral fins were thought to provide stabilization by counteracting the angle of the tail (Harris, 1936; Simanek & Thomson, 1977). However, fluid dynamics studies showed that the pectoral fins in several small-sized benthic and pelagic shark species do not produce vortices during steady swimming and thus do not help in the functioning to stabilize body movements (Wilga & Lauder, 2000, 2001; Maia *et al.*, 2012), rather these fins are mostly used for vertical maneuvers and banking turns (Wilga & Lauder, 2000, 2001). The anterior and almost horizontal insertion of the pectoral fins and the reduced ROM when compared to bony fishes are likely to limit the utility of these structures during steady swimming. The first dorsal fin can thus have a more prominent role in roll prevention.

The greater ROM of the second dorsal fin relative to the first dorsal fin in spiny dogfish, which is moving with the body, suggests that the second dorsal fin can have an active role in thrust production during steady swimming, contrary to the exclusive stabilizing role proposed by Harris (1936). In addition, the conformational changes between leading edge and trailing edge portions of the second dorsal fin were more pronounced than that for the first dorsal fin. This could be indicative of a dorsoventral cupping motion, which is characteristic of thrust producing fins (Standen & Lauder, 2005). EMG data on dorsal fin muscles confirm that the second dorsal fin is active. In a thrust producing structure, we would expect differences in onset and offset of left and right muscles, however this was not observed. This is likely explained by the fast cyclical contractions and independence of left and right dorsal fin muscles to the red epaxial muscle used as a reference. An alternative explanation would be that this fin is acting as a stabilizer, although the position of this fin far away from the center of mass and just preceding the caudal peduncle renders this unlikely.

The movement of the second dorsal fin in phase with the body axis indicates two potential roles for steady swimming in spiny dogfish: (1) the second dorsal fin moves passively with the caudal peduncle; or (2) the second dorsal fin actively undulates in phase with the caudal peduncle. In both cases the fin may be contributing to thrust production, in the first case by acting as an extension of the caudal peduncle and in the second case by actively cupping and creating thrust. Although we would expect alternating activity of the muscles in the second dorsal fin based on the kinematic analysis, our analysis of muscle activation did not verify this trend. However, muscle fibers were always recruited during steady swimming in a cyclical pattern, thus it is unlikely that this fin in solely passively moving with the tail.

Placement of the dorsal fins relative to the center of mass plays a role in determining fin function as a thruster or stabilizer by determining force orientation (Drucker & Lauder, 2001). In bluegill sunfish, a soft dorsal fin positioned posterior to the center of mass can impart thrust during steady swimming (Drucker & Lauder, 2001). In contrast, in rainbow and brook trout, the dorsal fin is placed closer to the center of the mass and the lateral component of thrust is larger, as expected (Drucker & Lauder, 2005; Standen & Lauder, 2007). The center of mass in adult spiny dogfish is located at approximately 33% of body length (Domenici *et al.*, 2004), where the first dorsal fin base is located (at 33.9% of the body length, Maia & Wilga, 2013*b*), while the second dorsal fin base is located at 64% of body length (A. Maia and C. A. Wilga, unpubl. data). Based on the short distance to the center of mass, the first dorsal fin is predicted to function mainly to counteract roll.

To the best of our knowledge, the activation pattern of dorsal fin muscles has only been investigated in bluegill sunfish (Jayne, Lozada & Lauder, 1996) and bamboo sharks (Maia & Wilga, 2013*a*). Bluegill sunfish have a spiny and a soft dorsal fin, with the soft portion located more posteriorly on the body. Motor activity data from the soft dorsal fin during steady swimming revealed these muscles to be recruited independently of red epaxial muscles (Jayne *et al.*, 1996), similarly to our study. In contrast to the present study, bamboo sharks alternate muscle activation between left and right sides for both first and second dorsal fins (Maia & Wilga, 2013*a*). This asynchronous bilateral activation suggests thrust production by the two dorsal fins, which in bamboo sharks are both placed on

the posterior half of the body (Maia & Wilga, 2013*a*). In contrast, spiny dogfish failed to show clear asynchronous activation patterns. Together with the more anterior placement of the first dorsal fin further support different functions of dorsal fins in distinct shark species.

No differences were detected for onset or duration of dorsal fin muscles activity on the same side of the fin in either of the dorsal fins. This was expected for spiny dogfish based on muscle arrangement of the dorsal fin, where there is only one continuous solid mass of muscle (Maia & Wilga, 2013*b*). Nonetheless, in bony fishes using labriform locomotion, which have individualized muscles to each fin ray, muscles on the same side of the pectoral fin are also simultaneously active during steady swimming (Drucker & Jensen, 1997; Westneat & Walker, 1997). This same pattern was also detected in leopard sharks during vertical maneuvers (Wilga & Lauder, 2001). Synchronous activation of multiple muscles on the same side might be necessary to counteract the strong hydrodynamic loads these fins experience. Fin morphology and biomechanical properties might be interacting with kinematics and muscle activation patterns to achieve a higher range of 3D conformation changes. Examples of biomechanical properties and muscle activation patterns interacting to increase fin mobility can be found in axial propulsion of swimming teleosts (McHenry, Pell & Long, 1995; Dickinson *et al.*, 2000).

Acknowledgements

The authors thank the Graduate School of Oceanography, Bonnie Witte, Ashley Stoehr, Ashley Heinze, and the Wilga Lab. George Lauder provided helpful discussion and Em Standen provided MATLAB code for graphical representations. The experiments were conducted under IACUC protocol # AN05-07-001. A. M. was funded by Fulbright-Portugal and Fundação para a Ciência e a Tecnologia (grant MCTES/FCT/SFRH/BD/36852/2007). CWG was funded by the National Science Foundation (grants IOS-0542177, IOS-0344126).

References

Arita, G.S. (1971). A re-examination of the functional morphology of the soft-rays in teleosts. *Copeia* **1971**, 691–697.

Benzer, P. (1944). Variations in the anatomy of the dorsal fins of Squalus acanthias. *Copeia* **1944**, 179–180.

Compagno, L.J.V. (1984). *Sharks of the World*. Rome: United Nations Development Program.

Compagno, L. (1999). Endoskeleton. In *Sharks, skates and rays – the biology of Elasmobranch Fishes*: 70–92. Hamlett, W.C. (Ed). Maryland: The Johns Hopkings University Press.

Dickinson, M.H., Farley, C.T., Full, R.J., Koehl, M.A.R., Kram, R. & Lehman, S. (2000). How animals move: an integrative view [Review]. *Science* **288**, 100–106.

Domenici, P., Standen, E.M., Levine, R.P., Marine, I. & Mardini, L.S. (2004). Escape manoeuvres in the spiny dogfish (*Squalus acanthias*). *J. Exp. Biol.* **207**, 2339–2349.

Donley, J. & Shadwick, R. (2003). Steady swimming muscle dynamics in the leopard shark *Triakis semifasciata*. *J. Exp. Biol.* **206**, 1117–1126.

Donley, J., Shadwick, R., Sepulveda, C.A., Konstantinidis, P. & Gemballa, S. (2005). Patterns of red muscle strain/activation and body kinematics during steady swimming in a lamnid shark, the shortfin mako (*Isurus oxyrinchus*). *J. Exp. Biol.* **208**, 2377–2387.

Drucker, E.G. & Jensen, J.S. (1997). Kinematic and electromyographic analysis of steady pectoral fin swimming in the surfperches. *J. Exp. Biol.* **200**, 1709–1723.

Drucker, E.G. & Lauder, G.V. (2001). Locomotor function of the dorsal fin in teleost fishes: experimental analysis of wake forces in sunfish. *J. Exp. Biol.* **204**, 2943–2958.

Drucker, E.G. & Lauder, G.V. (2005). Locomotor function of the dorsal fin in rainbow trout: kinematic patterns and hydrodynamic forces. *J. Exp. Biol.* **208**, 4479–4494.

Ferry, L.A. & Lauder, G.V. (1996). Heterocercal tail function in leopard sharks: a three dimensional kinematic analysis of two models. *J. Exp. Biol.* **199**, 2253–2268.

Fish, F.E. (2002). Balancing requirements for stability and maneuverability in cetaceans. *Integr. Comp. Biol.* **42**, 85–93.

Flammang, B.E. (2010). Functional morphology of the radialis muscle in shark tails. *J. Morphol.* **271**, 340–352.

Geerlink, P.J. (1987). The role of the pectoral fins in braking of mackerel, cod and saithe. *Neth. J. Zool.* **37**, 81–104.

Harris, J.E. (1936). The role of the fins in the equilibrium of the swimming fish. I. Wind tunnel tests on a model of Mustelus canis (Mitchell). *J. Exp. Biol.* **13**, 476–493.

Harris, J.E. (1937). The mechanical significance of the position and movements of the paired fins in the Teleostei. *Pap. Tortugas Lab.* **31**, 173–189.

Hedrick, T.L. (2008). Software techniques for two- and three-dimensional kinematic measurements of biological and biomimetic systems. *Bioinspir. Biomim.* **3**, 034001.

Jayne, B.C., Lozada, A.F. & Lauder, G.V. (1996). Function of the dorsal fin in bluegill sunfish: motor patterns during four distinct locomotor behaviors. *J. Morphol.* **228**, 307–326.

Lauder, G. (2006). Locomotion. In *The physiology of fishes* 3–46. Evans, D. & Claiborne, J. (Eds.), Boca Raton, FL: CRC Press.

Liem, K.F. & Summers, A.P. (1999). Muscular system – gross anatomy and functional morphology of muscles. In *Sharks, skates and rays - the biology of Elasmobranch Fishes*: 93–114. Hamlett, W.C. (Ed). Maryland: The Johns Hopkings University Press.

Lingham-Soliar, T. (2005). Caudal fin allometry in the white shark Carcharodon carcharias: implications for locomotory performance and ecology. *Naturwissenschaften* **92**, 231–236.

Maia, A. & Wilga, C.A. (2013a). Function of dorsal fins in bamboo shark during steady swimming. *Zoology (Jena)* **116**, 224–231.

Maia, A. & Wilga, C.D.A. (2013b). Anatomy and muscle activity of the dorsal fins in bamboo sharks and spiny dogfish during turning maneuvers. *J. Morphol.* **274**, 1288–1298.

Maia, A.M., Wilga, C.A. and Lauder, G.V. (2012). Locomotion in sharks, skates and rays. In *Biology of sharks and their relatives*: 125–152. Carrier, J.E., Musick, J.A. & Heithaus, M.R. (Eds.): Boca Raton, FL: CRC Press.

McHenry, M.J., Pell, C.A. & Long, J.H.J. (1995). Mechanical control of swimming speed: stiffness and axial wave form in undulating fish models. *J. Exp. Biol.* **198**, 2293–2305.

Roberts, T.J., Higginson, B.K., Nelson, F.E. & Gabaldon, A.M. (2007). Muscle strain is modulated more with running slope than speed in wild turkey knee and hip extensors. *J. Exp. Biol.* **210**, 2510–2517.

Schaeffer, B. & Williams, M. (1977). Relationship of fossil and living elasmobranchs. *Am. Zool.* **17**, 293–302.

Shirai, S. (1996). Phylogenetic Interrelationships of Neoselachians (Chondrichthyes: Euselachii). In *Interrelationships of fishes*: 9–34. Stiassney, M.L.J., Parenti, L.R. & Johnson, G.D. (Eds). San Diego: Academic Press.

Simanek, D.E. & Thomson, K.S. (1977). Body form and locomotion in sharks. *Am. Zool.* **17**, 343–354.

Simons, J.R. (1970). The direction of the thrust produced by the heterocercal tails of two dissimilar elasmobranchs: the Port Jackson shark, Heterodontus portusjacksoni (Meyer), and the piked dogfish, Squalusmegalops (Macleay). *J. Exp. Biol.* **52**, 95–107.

Standen, E. & Lauder, G. (2005). Dorsal and anal fin function in bluegill sunfish Lepomis macrochirus: three-dimensional kinematics during propulsion and maneuvering. *J. Exp. Biol.* **208**, 2753–2763.

Standen, E.M. & Lauder, G.V. (2007). Hydrodynamic function of dorsal and anal fins in brook trout (*Salvelinus fontinalis*). *J. Exp. Biol.* **210**, 325–339.

Tritico, H.M. & Cotel, A.J. (2010). The effects of turbulent eddies on the stability and critical swimming speed of creek chub (Semotilus atromaculatus). *J. Exp. Biol.* **213**, 2284–2293.

Webb, P.W. (2004). Response latencies to postural disturbances in three species of teleostean fishes. *J. Exp. Biol.* **207**, 955–961.

Webb, P.W. (2006). Stability and maneuverability. In *The physiology of fishes*: 281–332. Evans, D. & Claiborne. J. (Eds.) Boca Raton: CRC Press.

Webb, P.W. & Keyes, R.S. (1982). Swimming kinematics of sharks. *Fish. Bull.* **80**, 803–812.

Westneat, M.W. & Walker, J. (1997). Motor patterns of labriform locomotion: kinematic and electromyographic analysis of pectoral fin swimming in the labrid fish Gomphosus varius. *J. Exp. Biol.* **200**, 1881–1893.

Wilga, C.D. & Lauder, G.V. (2000). Hydrodynamics of the pectoral fins during locomotion in the leopard sharkTriakis semifasciata. *J. Exp. Biol.* **203**, 2261–2278.

Wilga, C.D. & Lauder, G.V. (2001). Functional morphology of the pectoral fins in bamboo sharks, Chiloscyllium plagiosum: Benthic vs. Pelagic station-holding. *J. Morphol.* **249**, 195–209.

Wilga, C.D. & Lauder, G.V. (2002). Function of the heterocercal tail in sharks: quantitative wake dynamics during steady horizontal swimming and vertical maneuvering. *J. Exp. Biol.* **205**, 2365–2374.

Wilga, C., & Lauder, G.V. (1999). Locomotion in sturgeon: function of the pectoral fins. *J. Exp. Biol.* **202**, 2413–2432.

Wilga, C.D. & Lauder, G.V. (2004). Biomechanics: hydrodynamic function of the shark's tail. *Nature* **430**, 850.

Zar, J.H. (2009). *Biostatistical analysis*. Upper Saddle River, NJ: Pearson.

Supporting Information

Additional Supporting Information may be found in the online version of this article:

Movie S1. Dorsal view of a spiny dogfish steadily swimming at 1BL.s^{-1}.